Editors' Suggestion

Near-Field Energy Transfer between Graphene and Magneto-Optic Media

Gaomin Tang,[1,*] Lei Zhang,[2,3] Yong Zhang,[4,5] Jun Chen,[6,†] and C. T. Chan[7]

[1]*Department of Physics, University of Basel, Klingelbergstrasse 82, CH-4056 Basel, Switzerland*
[2]*State Key Laboratory of Quantum Optics and Quantum Optics Devices, Institute of Laser Spectroscopy, Shanxi University, Taiyuan 030006, China*
[3]*Collaborative Innovation Center of Extreme Optics, Shanxi University, Taiyuan 030006, China*
[4]*School of Energy Science and Engineering, Harbin Institute of Technology, Harbin 150001, China*
[5]*Key Laboratory of Aerospace Thermophysics, Ministry of Industry and Information Technology, Harbin 150001, China*
[6]*State Key Laboratory of Quantum Optics and Quantum Optics Devices, Institute of Theoretical Physics, Shanxi University, Taiyuan 030006, China*
[7]*Department of Physics and Institute for Advanced Study, The Hong Kong University of Science and Technology, Hong Kong, China*

(Received 5 August 2021; accepted 19 November 2021; published 8 December 2021)

We consider the near-field radiative energy transfer between two separated parallel plates: graphene supported by a substrate and a magneto-optic medium. We first study the scenario in which the two plates have the same temperature. An electric current through the graphene gives rise to nonequilibrium fluctuations and induces energy transfer. Both the magnitude and direction of the energy flux can be controlled by the electric current and an in-plane magnetic field in the magneto-optic medium. This is due to the interplay between the nonreciprocal photon occupation number in the graphene and nonreciprocal surface modes in the magneto-optic plate. Furthermore, we report that a tunable thermoelectric current can be generated in the graphene in the presence of a temperature difference between the two plates.

DOI: 10.1103/PhysRevLett.127.247401

Introduction.—Nonreciprocity is attracting substantial interest in plasmonics and radiative energy harvesting. In magneto-optic materials, a magnetic field breaks time-reversal symmetry, which results in nonreciprocal electromagnetic surface waves. Owing to the broken reciprocity, various novel near-field heat transfer phenomena have been reported, including photon thermal Hall effect [1], persistent heat current [2,3], thermal magnetoresistance [4–7], thermal rectification [8], and Casimir heat engine [9,10].

In graphene, nonreciprocity can be induced by applying an electric current [11–15]. Interesting properties of graphene plasmons such as negative Landau damping [16] and Fizeau drag [17,18] have been studied. Current-biased graphene is in a nonequilibrium state, which leads to a finite photonic chemical potential [19] that depends on the in-plane wave vector $\mathbf{q}$ for the thermal electromagnetic radiation. The occupation number of radiative photons at angular frequency ω and electronic temperature T becomes nonreciprocal, $n(\omega) = [e^{\hbar(\omega-\mathbf{q}\cdot\mathbf{v}_d)/k_BT} - 1]^{-1}$, where $\mathbf{v}_d$ is the drift velocity of the electric current [20–23]. Regarding regulation of the photonic chemical potential, a p-n junction with a voltage bias has been reported to enable solid-state cooling in the near-field regime [24–26].

In this Letter, we study the near-field energy transfer between two parallel plates: graphene supported by a substrate and a magneto-optic plate [see Fig. 1(a)]. In the presence of an electric current through the graphene, a net energy is transferred between the plates when they have an equal electronic temperature. An in-plane magnetic field perpendicular to the electric current is applied to the magneto-optic medium. In the absence of the magnetic field, the energy flux flows from the graphene to the magneto-optic medium in the absence of a temperature difference between the plates. Remarkably, the energy flux direction can be controlled by the magnetic field due to the nonreciprocal surface modes of the magneto-optic medium. Furthermore, a tunable thermoelectric current can be generated in the graphene with a temperature difference between the two plates.

Formalism.—The system is schematically shown in Fig. 1(a) where the substrate, graphene, and magneto-optic plate are denoted by indices s, 1, and 2, respectively. Within the framework of fluctuational electrodynamics [27,28], the near-field radiative energy flux H on the magneto-optic plate is given by [29–32]

$$H = \int_0^\infty \frac{d\omega}{2\pi} \int_{c|\mathbf{q}|>\omega} \frac{d^2\mathbf{q}}{4\pi^2} \hbar\omega [n_{s2}\xi_{s2}(\omega,\mathbf{q}) + n_{12}\xi_{12}(\omega,\mathbf{q})], \tag{1}$$

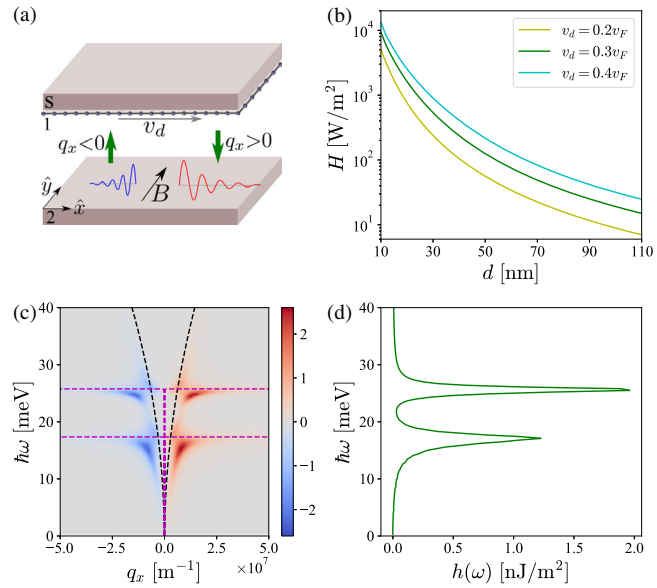

FIG. 1. (a) Schematic plot of the near-field energy transfer between graphene (1) supported by a substrate (s) and a magneto-optic medium plate (2) with air gap d. In the presence of an electric current with drift velocity v_d through the graphene, a net energy flux is transferred even when there is no temperature difference between the two plates. Its magnitude and direction can be modulated by the electric current and the magnetic field B applied to the magneto-optic medium. (b) Energy flux H versus d at different v_d with $B = 0$ and $T = 300$ K. (c) Energy transmission function $\mathcal{Z}$ (in units of meV) at $v_d = 0.3v_F$, $d = 20$ nm, and $q_y = 0$ against q_x and $\hbar\omega$. The black and magenta dashed lines are the dispersions of graphene plasmons and the surface modes of InSb at $B = 0$ in the absence of damping, respectively. (d) Spectrum $h(\omega)$ at $v_d = 0.3v_F$ and $d = 20$ nm.

where $\mathbf{q} = (q_x, q_y)$ is the in-plane wave vector and ω is the angular frequency. Here, $n_{ij} \equiv n_i - n_j$ is the occupation difference of the photons radiated from object i and j, with $i, j \in \{s, 1, 2\}$. Photonic transmission coefficients ξ_{s2} and ξ_{12} with air gap separation d are expressed as

$$\xi_{s2} = 4|\tau_1|^2 \mathrm{Im}(\rho_s)\mathrm{Im}(\rho_2)e^{-2k_z d}|u_{s1,2}|^2|u_{s,1}|^2, \quad (2)$$

$$\xi_{12} = 4\mathrm{Im}(\rho_{s1})\mathrm{Im}(\rho_2)e^{-2k_z d}|u_{s1,2}|^2 - \xi_{s2}, \quad (3)$$

with $k_z = \sqrt{|\mathbf{q}|^2 - (\omega/c)^2}$, $u_{s1,2} = (1 - \rho_{s1}\rho_2 e^{-2k_z d})^{-1}$, and $u_{s,1} = (1 - \rho_s\rho_1)^{-1}$. In the above, ρ_i is the reflection coefficient for the p-polarized mode of object i, and τ_1 is the transmission coefficient of the graphene which is treated as a thin film with finite thickness [33,34]. In addition, $\rho_{s1} = \rho_1 + \tau_1^2\rho_s u_{s,1}$ is the reflection coefficient of the graphene supported by the substrate. Details of these coefficients are provided in the Supplemental Material [35].

We now consider the scenario in which an electric current is applied through the graphene and all the objects have the same temperature T. In this case, n_{s2} vanishes, and Eq. (1) becomes

$$H = \int_0^\infty \frac{d\omega}{2\pi} \int_{c|\mathbf{q}|>\omega} \frac{d^2\mathbf{q}}{4\pi^2} \hbar\omega n_{12}(\omega, q_x)\xi_{12}(\omega, \mathbf{q}). \quad (4)$$

Without loss of generality, the electric current-induced drift velocity v_d in the graphene is along the positive direction of the x axis. The photon occupation number difference between the graphene and magneto-optic medium is thus [20–23,45,46]

$$n_{12}(\omega, q_x) = [e^{\hbar(\omega - q_x v_d)/k_B T} - 1]^{-1} - [e^{\hbar\omega/k_B T} - 1]^{-1}. \quad (5)$$

Equation (5) implies that the electric current results in a finite energy flux even in the absence of a temperature difference between the two plates. From Eqs. (4) and (5), a positive energy flux indicates that it flows from the graphene to the magneto-optic medium and inversely for a negative flux. In this work, we consider a gap separation d of not less than 10 nm so that the contribution from $\omega < q_x v_d$, which is only sizable with a subnanometer separation [21,22], can be neglected. For positive q_x, the energy transfer is from the graphene to the magneto-optic medium since n_{12} is positive under $\omega > q_x v_d$. For negative q_x, n_{12} is negative, and the energy transfer direction is opposite to that for positive q_x. We define the energy transmission function of the energy flux in Eq. (4) as

$$\mathcal{Z}(\omega, \mathbf{q}) = \hbar\omega n_{12}(\omega, q_x)\xi_{12}(\omega, \mathbf{q}), \quad (6)$$

which gives the energy transfer at given ω and $\mathbf{q}$. The energy flux spectrum $h(\omega)$ is defined through $H = \int_0^\infty d\omega h(\omega)/2\pi$.

For a three-dimensional object in the presence of magnetic field B, its dielectric tensor has off-diagonal elements due to the cyclotron motion at frequency $\omega_c = eB/m^*$, where m^* is the effective electron mass. Usually, the off-diagonal elements are negligible. In magneto-optic materials which have low carrier density and small effective mass, the cyclotron motion frequency ω_c can be comparable to the plasma frequency, which leads to large off-diagonal elements. Because of this, the surface modes of magneto-optic materials are nonreciprocal in the Voigt configuration. To study the interplay of the nonreciprocal effects from the photon occupation number and the surface modes, the magnetic field is applied along the y direction so that the dielectric tensor reads

$$\bar{\bar{\epsilon}}(\omega) = \begin{bmatrix} \epsilon_d & 0 & i\epsilon_a \\ 0 & \epsilon_p & 0 \\ -i\epsilon_a & 0 & \epsilon_d \end{bmatrix}, \quad (7)$$

with $\epsilon_a = \epsilon_\infty \omega_c \omega_p^2 / \{\omega[(\omega + i\gamma)^2 - \omega_c^2]\}$ using the Drude model. Here, ϵ_∞ is the high-frequency dielectric constant,

ω_p is the plasma frequency, and γ describes the free-carrier damping constant. The expressions of ϵ_d and ϵ_p are given in the Supplemental Material [35]. The dispersion relation of p-polarized surface modes with wave vector q_x is [36]

$$\epsilon_v\sqrt{(\omega/c)^2-q_x^2}+\sqrt{\epsilon_v(\omega/c)^2-q_x^2}-i\epsilon_a q_x/\epsilon_d=0, \quad (8)$$

with $\epsilon_v=\epsilon_d-\epsilon_a^2/\epsilon_d$. This expression explicitly indicates that ϵ_a gives rise to the nonreciprocal dispersion.

In magnetic Weyl semimetals, Weyl-node separation in momentum space leads to the anomalous Hall effect [47–49] such that there are off-diagonal components in the dielectric tensor. Compared to magneto-optic materials, magnetic Weyl semimetals intrinsically support nonreciprocal surface polaritons [50,51]. Therefore, the magneto-optic medium can be replaced by a magnetic Weyl semimetal such that an external magnetic field is not needed [7,37,52–54].

In the numerical calculation, we choose hexagonal boron nitride as the substrate. The chemical potential of the graphene is 0.1 eV. The drift velocity in the graphene is set to around $0.3v_F$ so that the nonreciprocity of the graphene plasmons can be neglected [11]. This can be seen from the black dashed lines in Fig. 1(c). The magneto-optic medium is chosen to be InSb. The contribution from the term ξ_{s2} in ξ_{12} given by Eq. (3) is negligible due to the mismatch between the surface modes from the hexagonal boron nitride and InSb. Below, we separately discuss the scenarios in the absence and presence of a magnetic field at $T=300$ K.

Energy transfer at $B=0$.—Figure 1(b) shows the energy flux versus gap separation d in the absence of a magnetic field. The positive value of the energy flux is explained as follows. Under $B=0$, the surface polaritons of the InSb plate are reciprocal, as is the transmission coefficient ξ_{12}. Because $n_{12}(\omega,q_x)>-n_{12}(\omega,-q_x)$ for $\omega>q_xv_d$ with $q_x>0$, the energy transfer of the positive q_x dominates over that of the negative q_x, and the net energy flux is from the graphene to the InSb plate. This argument is supported by the energy transmission function $\mathcal{Z}$ in Fig. 1(c) and the spectrum $h(\omega)$ in Fig. 1(d). The two positive peaks in the spectrum correspond to the two surface-polariton frequencies of InSb and are due to the difference between the contributions from positive and negative q_x. Figure 1(b) shows that the energy flux decreases with increasing separation d, which is due to the evanescent nature of the surface modes.

Energy transfer at finite B.—We now consider the situation in which a magnetic field $\mathbf{B}=B\hat{y}$ is applied to the magneto-optic plate. Positive and negative magnetic fields B are defined as being along the positive and negative directions of the y axis, respectively. For $B>0$, the dispersion of the surface polaritons in the magneto-optic plate is redshifted for positive q_x and experiences a blueshift for negative q_x compared to the dispersion in the absence of a magnetic field [55]. This scenario is opposite for $B<0$. The surface polaritons of the InSb plate for positive and negative $\mathrm{Re}(q_x)$ at $B=4$ T are shown in Fig. 2(a). Here, q_x is complex because the damping constants are taken into account in Eq. (8). The polaritons at $\mathrm{Re}(q_x)<0$ are more strongly damped than those at $\mathrm{Re}(q_x)>0$. For the case with reciprocal surface modes and photonic transmission coefficients, the energy transfer of $n_{12}(\omega,q_x)$ with $q_xv_d>0$ dominates over that of $n_{12}(\omega,-q_x)$, which leads to the net energy flux flowing out of the graphene sheet. However, because of the nonreciprocal surface polaritons of the magneto-optic medium, the photonic transmission coefficients are different for wave vectors of (q_x,q_y) and $(-q_x,q_y)$. This enables the net energy flux direction to be changed by a magnetic field.

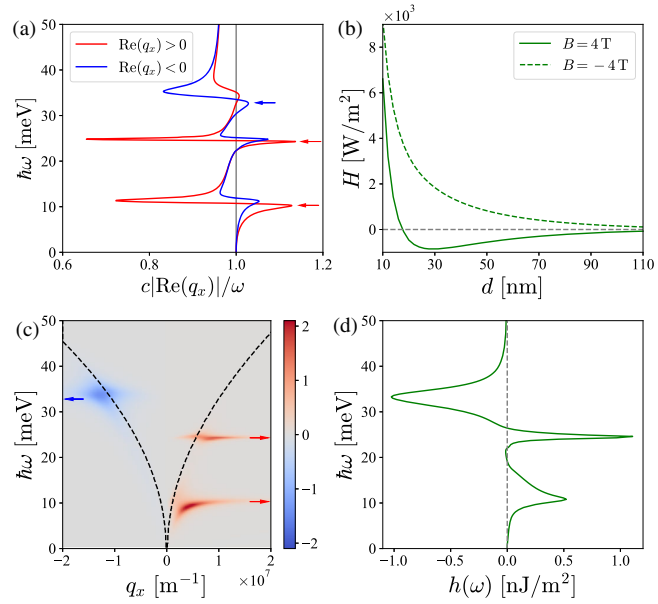

FIG. 2. (a) Dispersion of the surface modes of InSb in the Voigt configuration at $B=4$ T. (b) Energy flux H versus separation d at $B=4$ and $B=-4$ T with $v_d=0.3v_F$ and $T=300$ K. (c) Energy transmission function $\mathcal{Z}$ (in units of meV) at $B=4$ T, $d=50$ nm, and $q_y=0$ against q_x and $\hbar\omega$. The black dashed lines are dispersions of the graphene plasmons. The energies $\hbar\omega$ indicated by the arrows are the same as the corresponding energies indicated in (a). (d) Spectrum $h(\omega)$ at $B=4$ T and $d=50$ nm.

Figure 2(b) shows the energy flux versus the gap separation at $B=4$ (solid line) and $B=-4$ T (dashed line) with $v_d=0.3v_F$. At $B=4$ T, the energy flux is negative when the gap separation is larger than about 18 nm. To understand this, we show the energy transmission function in Fig. 2(c) and the energy flux spectrum $h(\omega)$ in Fig. 2(d) at $B=4$ T and $d=50$ nm. The energies $\hbar\omega$ around which the energy transfer is prominent are indicated by arrows in Fig. 2(c). The arrows correspond to the peaks in Fig. 2(d). The contributions from the positive

and negative q_x give rise to the positive and negative peaks, respectively. The negative peak is broader than the two positive peaks, which originates from the nonreciprocity of the surface polaritons of InSb. Therefore, the increased polariton damping at negative q_x and decreased damping at positive q_x give rise to the negative energy flux at $B = 4$ T and $d \gtrsim 18$ nm. The energy flux is positive at $B = 4$ T and $d \lesssim 18$ nm since the nonreciprocity of the photon occupation from the graphene increases with increasing magnitude of wave vector q_x. Thus, the interplay between the nonreciprocal photon occupation number and the nonreciprocal surface modes governs the net energy transfer direction. For $B = -4$ T, surface polariton broadening of InSb occurs at positive q_x such that the synergy from the nonreciprocal effects of the photon occupation number and the surface polaritons gives rise to the positive energy flux in Fig. 2(b).

The energy flux versus magnetic field B behavior at $d = 50$ nm is displayed in Fig. 3. The energy flux vanishes at certain magnetic fields, which are denoted as B_-, B_1 and B_2 for $v_d = 0.3v_F$. Under a small magnetic field ($0 < B < B_1$), the nonreciprocity of the surface modes of InSb is weak such that the energy transfer direction is dominated by the nonreciprocity of the photon occupation in the graphene and is from the graphene to the InSb plate. With increasing magnetic field, the energy flux first becomes negative ($B_1 < B < B_2$) and then positive ($B > B_2$). The negative value of the energy flux can be explained in the same way as that at $B = 4$ T in Fig. 2(b). For $B \leq 0$, with increasing magnetic field magnitude, the energy flux first increases and then decreases, finally becoming negative. The region of positive energy flux can be explained similarly to that at $B = -4$ T in Fig. 2(b).

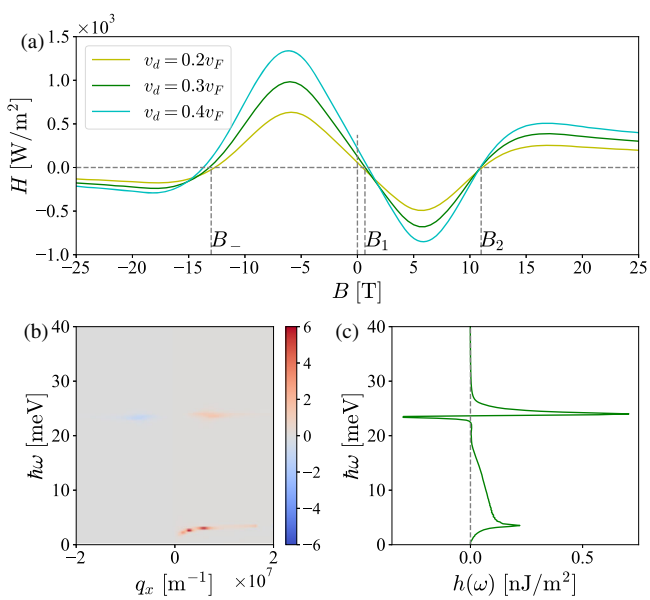

FIG. 3. (a) Energy flux H versus magnetic field B at different drift velocities v_d with $d = 50$ nm and $T = 300$ K. (b) Energy transmission function $\mathcal{Z}$ at $q_y = 0$, $B = 18$ T, $v_d = 0.3v_F$, and $d = 50$ nm against q_x and $\hbar\omega$. (c) Spectrum $h(\omega)$ at $B = 18$ T and $v_d = 0.3v_F$.

When the magnetic field is sufficiently large, the surface polaritons in InSb become highly nonreciprocal. For a large positive magnetic field, the surface waves at $q_x < 0$ are strongly damped such that their contribution to the energy transfer is suppressed. Therefore, the energy transfer contribution from $q_x > 0$ dominates over that from $q_x < 0$ above a certain magnetic field [B_2 at $v_d = 0.3v_F$ in Fig. 3(a)], which leads to a net energy flow from the graphene to the InSb plate. This explanation is supported by Figs. 3(b) and 3(c). For a large magnetic field along the negative y axis [$B < B_-$ in Fig. 3(a)], the contribution from $q_x < 0$ is dominant, which leads to a negative energy flux.

In the above, we have discussed the scenario in which the in-plane magnetic field is perpendicular to the electric current. When the magnetic field is parallel to the electric current, the surface polaritons of the magneto-optic medium are reciprocal along the direction of the electric current. In this case, the net energy transfer is from the graphene to the magneto-optic medium since there is no interplay between the nonreciprocal effects.

Notably, our findings do not violate the second law of thermodynamics. Energy could possibly be transferred from one body to another at a higher temperature if there is an external agent. This can be applied to our case in which the two bodies have the same temperature, as an external agent is needed to maintain the electric current in the graphene.

Thermoelectric effect.—The phenomena discussed above imply a thermoelectric effect. We consider the same setup with a temperature difference between the two plates, and no external electric current is applied to the graphene. In this case, we have $n_{s2} = n_{12}$, and the heat flux is expressed by

$$H = \int_0^\infty \frac{d\omega}{2\pi} \int_{c|\mathbf{q}|>\omega} \frac{d^2\mathbf{q}}{4\pi^2} \hbar\omega n_{12}(\omega)[\xi_{12}(\omega, \mathbf{q}) + \xi_{s2}(\omega, \mathbf{q})], \tag{9}$$

with $n_{12}(\omega) = (e^{\hbar\omega/k_B T_1} - 1)^{-1} - (e^{\hbar\omega/k_B T_2} - 1)^{-1}$. Here, T_1 and T_2 are the temperatures of the graphene plate and InSb, respectively. When a magnetic field is applied along the y axis in the InSb plate, the heat transfer rates at momenta q_x and $-q_x$ are different such that the electrons in the graphene of momenta q_x and $-q_x$ have different occupations [see Fig. 4]. When the impurity scattering in the graphene is weak, this occupation difference can induce an electric current along the x direction in the graphene due to its high electron mobility. The magnitude and direction of the induced electric current can be controlled by the magnetic field. Thus, the near-field thermoelectric effect can be achieved. In the absence of a magnetic field, the in-plane isotropy is preserved such that an in-plane electric

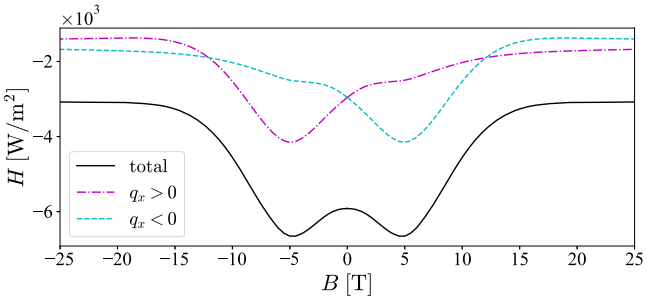

FIG. 4. Heat flux H versus magnetic field B at $T_1 = 300$ K, $T_2 = 330$ K, and $d = 50$ nm (solid line). The contributions to the heat flux from positive q_x (dash-dotted line) and negative q_x (dashed line) are plotted separately. The negative heat flux indicates that the heat flows from the InSb plate to the graphene.

current cannot be generated. The thermoelectric effect is analogous to the Casimir heat engine in Refs. [9,10], where the thermal energy is converted into mechanical work. Notably, the thermoelectric effect in this work is different from that in the traditional near-field thermophotovoltaic cell using a p-n junction [56].

To conclude, we have studied the near-field energy transfer between graphene and magneto-optic media. The energy transfer is induced by the electric current through the graphene in the absence of a temperature difference. Its direction and magnitude can be tuned by the electric current and the in-plane magnetic field in the magneto-optic medium. The tunability of the direction is due to the interplay between the nonreciprocal photon occupation number from the graphene and the nonreciprocal surface modes of the magneto-optic medium. We have also proposed a form of the near-field thermoelectric effect in which the electric current can be generated using nonreciprocal surface modes. Our work paves a new route toward nanoscale energy and thermal management and harvesting using nonreciprocity.

G. T. acknowledges financial support from the Swiss National Science Foundation (SNSF) and the NCCR Quantum Science and Technology. L. Z. and J. C. acknowledge support from the National Natural Science Foundation of China (Grants No. 12174231, No. 12074230, No. 12047571), National Key R&D Program of China under Grants No. 2017YFA0304203, 1331KSC, and Shanxi Province 100-Plan Talent Program. Y. Z. acknowledges support from the National Natural Science Foundation of China (Grant No. 52076056). C. T. C. acknowledges support from the Hong Kong RGC (16303119).

*gaomin.tang@unibas.ch
†chenjun@sxu.edu.cn

[1] P. Ben-Abdallah, Photon Thermal Hall Effect, Phys. Rev. Lett. **116**, 084301 (2016).
[2] L. Zhu and S. Fan, Persistent Directional Current at Equilibrium in Nonreciprocal Many-Body near Field Electromagnetic Heat Transfer, Phys. Rev. Lett. **117**, 134303 (2016).
[3] L. Zhu, Y. Guo, and S. Fan, Theory of many-body radiative heat transfer without the constraint of reciprocity, Phys. Rev. B **97**, 094302 (2018).
[4] E. Moncada-Villa, V. Fernández-Hurtado, F. J. García-Vidal, A. García-Martín, and J. C. Cuevas, Magnetic field control of near-field radiative heat transfer and the realization of highly tunable hyperbolic thermal emitters, Phys. Rev. B **92**, 125418 (2015).
[5] I. Latella and P. Ben-Abdallah, Giant Thermal Magnetoresistance in Plasmonic Structures, Phys. Rev. Lett. **118**, 173902 (2017).
[6] R. M. Abraham Ekeroth, P. Ben-Abdallah, J. C. Cuevas, and A. García-Martín, Anisotropic thermal magnetoresistance for an active control of radiative heat transfer, ACS Photonics **5**, 705 (2018).
[7] C. Guo, B. Zhao, D. Huang, and S. Fan, Radiative thermal router based on tunable magnetic Weyl semimetals, ACS Photonics **7**, 3257 (2020).
[8] A. Ott and S.-A. Biehs, Thermal rectification and spin-spin coupling of nonreciprocal localized and surface modes, Phys. Rev. B **101**, 155428 (2020).
[9] D. Gelbwaser-Klimovsky, N. Graham, M. Kardar, and M. Krüger, Near Field Propulsion Forces from Nonreciprocal Media, Phys. Rev. Lett. **126**, 170401 (2021).
[10] C. Khandekar, S. Buddhiraju, P. R. Wilkinson, J. K. Gimzewski, A. W. Rodriguez, C. Chase, and S. Fan, Nonequilibrium Casimir effects of nonreciprocal surface waves, arXiv:2106.10584.
[11] D. S. Borgnia, T. V. Phan, and L. S. Levitov, Quasi-relativistic Doppler effect and non-reciprocal plasmons in graphene, arXiv:1512.09044.
[12] B. V. Duppen, A. Tomadin, A. N. Grigorenko, and M. Polini, Current-induced birefringent absorption and nonreciprocal plasmons in graphene, 2D Mater. **3**, 015011 (2016).
[13] T. A. Morgado and M. G. Silveirinha, Drift-induced unidirectional graphene plasmons, ACS Photonics **5**, 4253 (2018).
[14] T. A. Morgado and M. G. Silveirinha, Nonlocal effects and enhanced nonreciprocity in current-driven graphene systems, Phys. Rev. B **102**, 075102 (2020).
[15] M. Papaj and C. Lewandowski, Plasmonic Nonreciprocity Driven by Band Hybridization in Moiré Materials, Phys. Rev. Lett. **125**, 066801 (2020).
[16] T. A. Morgado and M. G. Silveirinha, Negative Landau Damping in Bilayer Graphene, Phys. Rev. Lett. **119**, 133901 (2017).
[17] Y. Dong, L. Xiong, I. Y. Phinney, Z. Sun, R. Jing, A. S. McLeod, S. Zhang, S. Liu, F. L. Ruta, H. Gao, Z. Dong, R. Pan, J. H. Edgar, P. Jarillo-Herrero, L. S. Levitov, A. J. Millis, M. M. Fogler, D. A. Bandurin, and D. N. Basov, Fizeau drag in graphene plasmonics, Nature (London) **594**, 513 (2021).
[18] W. Zhao, S. Zhao, H. Li, S. Wang, S. Wang, M. I. B. Utama, S. Kahn, Y. Jiang, X. Xiao, S. Yoo, K. Watanabe, T. Taniguchi, A. Zettl, and F. Wang, Efficient Fizeau drag from Dirac electrons in monolayer graphene, Nature (London) **594**, 517 (2021).

[19] C. H. Henry and R. F. Kazarinov, Quantum noise in photonics, Rev. Mod. Phys. **68**, 801 (1996).

[20] A. I. Volokitin and B. N. J. Persson, Theory of the interaction forces and the radiative heat transfer between moving bodies, Phys. Rev. B **78**, 155437 (2008).

[21] A. I. Volokitin and B. N. J. Persson, Quantum Friction, Phys. Rev. Lett. **106**, 094502 (2011).

[22] A. I. Volokitin and B. N. J. Persson, Near-field radiative heat transfer between closely spaced graphene and amorphous SiO_2, Phys. Rev. B **83**, 241407(R) (2011).

[23] J. Peng and J.-S. Wang, Current-induced heat transfer in double-layer graphene, arXiv:1805.09493.

[24] K. Chen, P. Santhanam, S. Sandhu, L. Zhu, and S. Fan, Heat-flux control and solid-state cooling by regulating chemical potential of photons in near-field electromagnetic heat transfer, Phys. Rev. B **91**, 134301 (2015).

[25] K. Chen, P. Santhanam, and S. Fan, Near-Field Enhanced Negative Luminescent Refrigeration, Phys. Rev. Applied **6**, 024014 (2016).

[26] L. Zhu, A. Fiorino, D. Thompson, R. Mittapally, E. Meyhofer, and P. Reddy, Near-field photonic cooling through control of the chemical potential of photons, Nature (London) **566**, 239 (2019).

[27] S. M. Rytov, *Theory of Electrical Fluctuation and Thermal Radiation* (Academy of Science of USSR, Moscow, 1953).

[28] D. Polder and M. Van Hove, Theory of radiative heat transfer between closely spaced bodies, Phys. Rev. B **4**, 3303 (1971).

[29] R. Messina, M. Antezza, and P. Ben-Abdallah, Three-Body Amplification of Photon Heat Tunneling, Phys. Rev. Lett. **109**, 244302 (2012).

[30] R. Messina and M. Antezza, Three-body radiative heat transfer and Casimir-Lifshitz force out of thermal equilibrium for arbitrary bodies, Phys. Rev. A **89**, 052104 (2014).

[31] I. Latella, P. Ben-Abdallah, S.-A. Biehs, M. Antezza, and R. Messina, Radiative heat transfer and nonequilibrium Casimir-Lifshitz force in many-body systems with planar geometry, Phys. Rev. B **95**, 205404 (2017).

[32] S.-A. Biehs, R. Messina, P. S. Venkataram, A. W. Rodriguez, J. C. Cuevas, and P. Ben-Abdallah, Near-field radiative heat transfer in many-body systems, Rev. Mod. Phys. **93**, 025009 (2021).

[33] A. Vakil and N. Engheta, Transformation optics using graphene, Science **332**, 1291 (2011).

[34] M. Lim, S. S. Lee, and B. J. Lee, Near-field thermal radiation between graphene-covered doped silicon plates, Opt. Express **21**, 22173 (2013).

[35] See Supplemental Material at http://link.aps.org/supplemental/10.1103/PhysRevLett.127.247401 for details of the numerical calculation, which includes Refs. [11,12,14,16,23,29,30,33,34,36–44].

[36] B. Hu, Y. Zhang, and Q. J. Wang, Surface magneto plasmons and their applications in the infrared frequencies, Nanophotonics **4**, 383 (2015).

[37] G. Tang, J. Chen, and L. Zhang, Twist-induced control of near-field heat radiation between magnetic Weyl semimetals, ACS Photonics **8**, 443 (2021).

[38] D. Svintsov and V. Ryzhii, Comment on "Negative Landau Damping in Bilayer Graphene", Phys. Rev. Lett. **123**, 219401 (2019).

[39] T. Zhu, M. Antezza, and J.-S. Wang, Dynamical polarizability of graphene with spatial dispersion, Phys. Rev. B **103**, 125421 (2021).

[40] T. A. Morgado and M. G. Silveirinha, Morgado and Silveirinha Reply, Phys. Rev. Lett. **123**, 219402 (2019).

[41] A. Kumar, T. Low, K. H. Fung, P. Avouris, and N. X. Fang, Tunable light–matter interaction and the role of hyperbolicity in graphene–hBN system, Nano Lett. **15**, 3172 (2015).

[42] P. A. D. Gonçalves and N. M. R. Peres, *An Introduction to Graphene Plasmonics* (World Scientific, Singapore, 2016).

[43] E. D. Palik, R. Kaplan, R. W. Gammon, H. Kaplan, R. F. Wallis, and J. J. Quinn, Coupled surface magnetoplasmon-optic-phonon polariton modes on InSb, Phys. Rev. B **13**, 2497 (1976).

[44] K. W. Chiu and J. J. Quinn, Magneto-plasma surface waves in solids, Il Nuovo Cimento B (1971–1996) **10**, 1 (1972).

[45] A. I. Volokitin and B. N. J. Persson, Near-field radiative heat transfer and noncontact friction, Rev. Mod. Phys. **79**, 1291 (2007).

[46] M. F. Maghrebi, R. Golestanian, and M. Kardar, Quantum Cherenkov radiation and noncontact friction, Phys. Rev. A **88**, 042509 (2013).

[47] E. Liu, Y. Sun, N. Kumar, L. Muechler, A. Sun, L. Jiao, S.-Y. Yang, D. Liu, A. Liang, Q. Xu, J. Kroder, V. Süß, H. Borrmann, C. Shekhar, Z. Wang, C. Xi, W. Wang, W. Schnelle, S. Wirth, Y. Chen, S. T. B. Goennenwein, and C. Felser, Giant anomalous Hall effect in a ferromagnetic kagome-lattice semimetal, Nat. Phys. **14**, 1125 (2018).

[48] R. Singha, S. Roy, A. Pariari, B. Satpati, and P. Mandal, Magnetotransport properties and giant anomalous Hall angle in the half-Heusler compound TbPtBi, Phys. Rev. B **99**, 035110 (2019).

[49] P. Li, J. Koo, W. Ning, J. Li, L. Miao, L. Min, Y. Zhu, Y. Wang, N. Alem, C.-X. Liu, Z. Mao, and B. Yan, Giant room temperature anomalous Hall effect and tunable topology in a ferromagnetic topological semimetal Co_2MnAl, Nat. Commun. **11**, 3476 (2020).

[50] J. Hofmann and S. Das Sarma, Surface plasmon polaritons in topological Weyl semimetals, Phys. Rev. B **93**, 241402 (R) (2016).

[51] O. V. Kotov and Y. E. Lozovik, Giant tunable nonreciprocity of light in Weyl semimetals, Phys. Rev. B **98**, 195446 (2018).

[52] B. Zhao, C. Guo, C. A. C. Garcia, P. Narang, and S. Fan, Axion-field-enabled nonreciprocal thermal radiation in Weyl semimetals, Nano Lett. **20**, 1923 (2020).

[53] Y. Tsurimaki, X. Qian, S. Pajovic, F. Han, M. Li, and G. Chen, Large nonreciprocal absorption and emission of radiation in type-I Weyl semimetals with time reversal symmetry breaking, Phys. Rev. B **101**, 165426 (2020).

[54] S. Pajovic, Y. Tsurimaki, X. Qian, and G. Chen, Intrinsic nonreciprocal reflection and violation of Kirchhoff's law of radiation in planar type-I magnetic Weyl semimetal surfaces, Phys. Rev. B **102**, 165417 (2020).

[55] C. Khandekar and Z. Jacob, Thermal spin photonics in the near-field of nonreciprocal media, New J. Phys. **21**, 103030 (2019).

[56] E. Tervo, E. Bagherisereshki, and Z. Zhang, Near-field radiative thermoelectric energy converters: A review, Front. Energy **12**, 5 (2018).